Chemistry Europe

AWARD

Nominate a Worthy Chemist Chemistry Europe Award

Subject:
chemistry for sustainability, energy, materials, environment

Consists of:
prize money amounting to EUR 10,000, certificate

Deadline:
November 1, 2022

Click here for more info & nomination

ChemPubSoc Europe

DOI: 10.1002/slct.201903886

Chemistry SELECT Full Papers

Medicinal Chemistry & Drug Discovery

A Novel Class Substituted Imidazo[2,1-*b*][1,3,4]thiadiazole Derivatives: Synthesis, Characterization, In Vitro Biological Activity, and Potential Inhibitors Design Studies

Mustafa Er,*[a] Farid Ahmadov,[a] Tuncay Karakurt,[b] Şahin Direkel,[c] and Hakan Tahtaci[a]

In this study, imidazo[2,1-*b*][1,3,4]thiadiazole derivatives were designed and synthesized. All of the synthesized compounds were characterized by ^{1}H and ^{13}C nuclear magnetic resonance (^{1}H NMR and ^{13}C NMR), fourier-transform infrared spectroscopy (FT-IR), elemental analysis, mass spectrometry, and X-ray diffraction.

The synthesized compounds were tested for antileishmanial activity against two *Leishmania* species and antibacterial activity against nine bacterial species in the study. It was observed that 2-(4-Fluorobenzylthio)-6-(4-fluorophenyl)imidazo [2,1-*b*][1,3,4]thiadiazole (**5**) had the highest antileishmanial activity (MIC: 625 μg/mL). Also, 4-(2-(4-fluorobenzylthio)imidazo [2,1-*b*][1,3,4]thiadiazol-6-yl)benzonitrile (**10**), 2-(4-fluorobenzylthio)-6-(4-phenylphenyl)imidazo[2,1-*b*][1,3,4]thiadiazole (**11**), and 4-(2-(4-methoxybenzyl)imidazo[2,1-*b*][1,3,4]thiadiazol-6-yl) benzonitrile (**25**) were found to be effective at different studied concentrations.

PyRx software, which uses a Lamarckian genetics algorithm, was utilized to find the affinity values of all compounds in molecular docking simulations. Pharmacokinetic properties and toxicities of the ligands were then researched using PROTOX (a webserver for the prediction of oral toxicities of small molecules) and FAF-Drugs (free adsorption distribution, metabolism, excretion (ADME) tox filtering tool). The study showed that the ligands had acceptable toxicity and ADME properties for the inhibition of the 3JUS receptor.

Introduction

It has long been known that heterocyclic aromatic compounds have many biological activities.

Among the most commonly used heterocyclic compounds in pharmaceutics and clinical drugs are imidazole, 1,3,4-thiadiazole and their derivatives. These heterocyclic systems, in which imidazole and 1,3,4-thiadiazole rings are fused to each other with a bridgehead nitrogen atom, are referred to as imidazo[2,1-*b*][1,3,4]thiadiazoles.[1]

Imidazo[2,1-*b*][1,3,4]thiadiazole derivatives, which contain nitrogen and sulfur atoms in their heterocyclic structure, have been shown to exhibit various biological activities such as antifungal,[1,2] anticancer,[3] antihyperlipidemic,[3] antimicrobial,[4–7] anti-inflammatory,[8,9] antituberculosis,[10–13] anticonvulsant,[14] analgesic,[14] and diuretic activities.[15] Numerous chemical and medical studies were conducted on imidazo [2,1-*b*][1,3,4]thiadiazole derivatives because of their various biological activites. Therefore, imidazo[2,1-*b*][1,3,4]thiadiazole and their derivatives have become important compounds commonly studied in the pharmaceutical chemistry and industry.[16,17]

Another reason for the scientific interest in imidazo[2,1-*b*] [1,3,4]thiadiazole derivatives is the good antibacterial activity of these compounds.[1,17] Since their discovery in the early 20th century, antibiotics have been widely used in the treatment of bacterial infections. Uninformed and excessive use of anti-

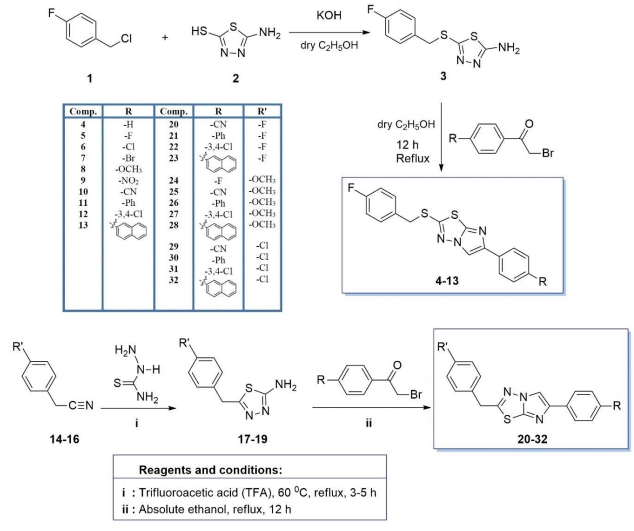

Scheme 1. Synthetic route for the synthesis of substituted imidazo[2,1-*b*] [1,3,4]thiadiazole derivatives (**4-13** and **20–32**).

[a] *Prof. M. Er, F. Ahmadov, Dr. H. Tahtaci*
Department of Chemistry, Faculty of Science, Karabuk University, 78050, Karabuk, Turkey
Tel: +90 370 418 72 60
Fax: +90 370 418 72 62
E-mail: mustafaer@karabuk.edu.tr

[b] *Dr. T. Karakurt*
Department of Chemical Engineering, Faculty of Engineering and Architecture, Kırşehir Ahi Evran University, 40100, Kırşehir, Turkey

[c] *Dr. Ş. Direkel*
Department of Medical Microbiology, Faculty of Medicine, Giresun University, Giresun, 28100, Turkey

Supporting information for this article is available on the WWW under https://doi.org/10.1002/slct.201903886

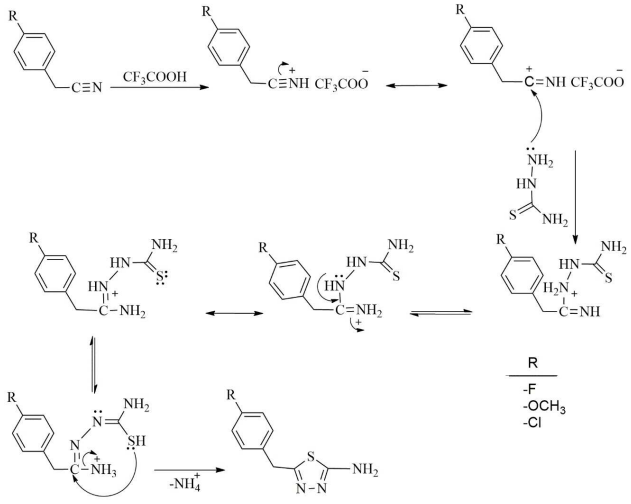

Scheme 2. The mechanism of the formation of 2-amino-1,3,4-thiadiazole derivatives (**17-19**).

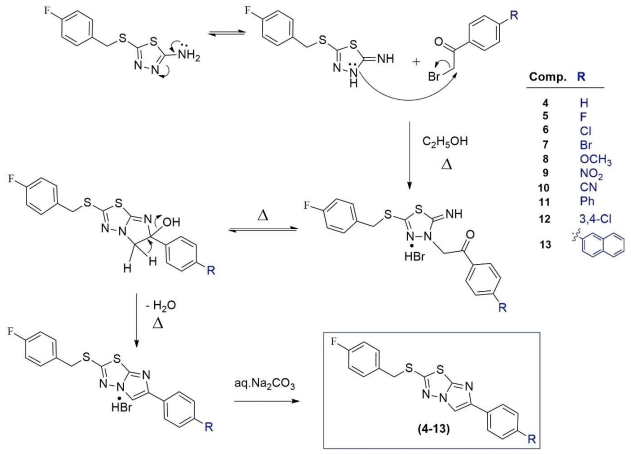

Scheme 3. Formation mechanism of imidazo[2,1-*b*][1,3,4]thiadiazole derivatives (**4-13**).

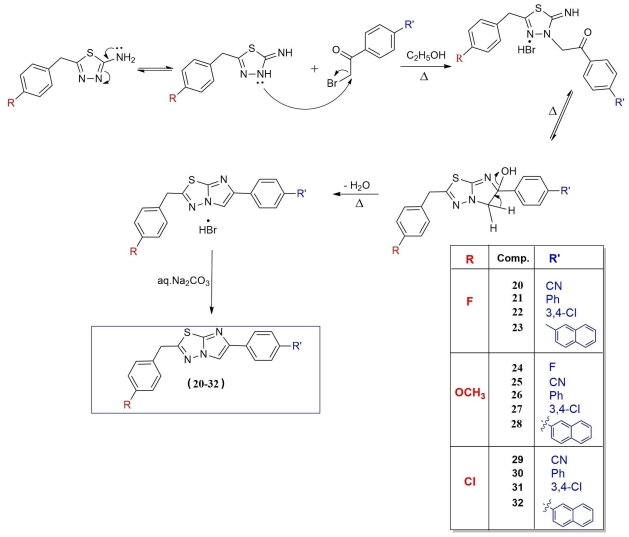

Scheme 4. Formation mechanism of imidazo[2,1-*b*][1,3,4]thiadiazole derivatives (**20-32**).

Table 1. The minimum inhibitory concentration (MIC) values of the compounds and the reference drug (Amphotericin B) against *Leishmania infantum* and *Leishmania tropica* promastigotes.

Compounds	*L.infantum* MIC Values (μg/ml)	*L.tropica* MIC Values (μg/ml)
4	>10,000	>10,000
5	625	625
6	>10,000	>10,000
7	>10, 000	>10,000
8	>10,000	>10,000
9	>10,000	>10,000
10	10,000	10,000
11	10,000	5,000
12	>10,000	>10,000
13	>10,000	>10,000
20	>10,000	>10,000
21	>10,000	>10,000
22	>10,000	>10,000
23	>10,000	>10,000
24	>10,000	>10,000
25	10,000	>10,000
26	>10,000	>10,000
27	>10,000	>10,000
28	>10,000	>10,000
29	>10,000	>10,000
30	>10,000	>10,000
31	>10,000	>10,000
32	>10,000	>10,000
Amphotericin B	<312	<312

biotics, which traditionally show their effects by killing or inhibiting the reproduction of bacteria, leads to the emergence of pathogens that are resistant against them. Moreover, prolonged use of antibiotics may lead to the disappearance of beneficial bacteria found in the human body as normal flora elements or may transform them into harmful bacteria. Bacterial infections cause approximately 16 million deaths annually. Therefore, it is necessary to design new antibacterial drugs to provide protection against possible pandemics. Various active ingredients that show antibacterial activity have been developed with advancing technology and these ingredients are now used to treat various bacterial infections.[18,19]

Leishmaniasis is a disease caused by the protozoan *Leishmania* parasite found in infected female sand flies. The disease is usually seen in regions where financial resources are limited and poverty, malnutrition, and weak immunity are rampant. It is estimated that 700,000 to 1 million new cases occur annually, while 26,000 to 65,000 deaths occur in association with the disease.[20]

In light of the literature data, this study aims to synthesize novel imidazo[2,1-*b*][1,3,4]thiadiazole derivatives (**4-13** and **20–32**), characterize them, and investigate their antileishmanial and antibacterial activities.

Another purpose of this study is to reveal whether or not the synthesized compounds could be used as drugs via

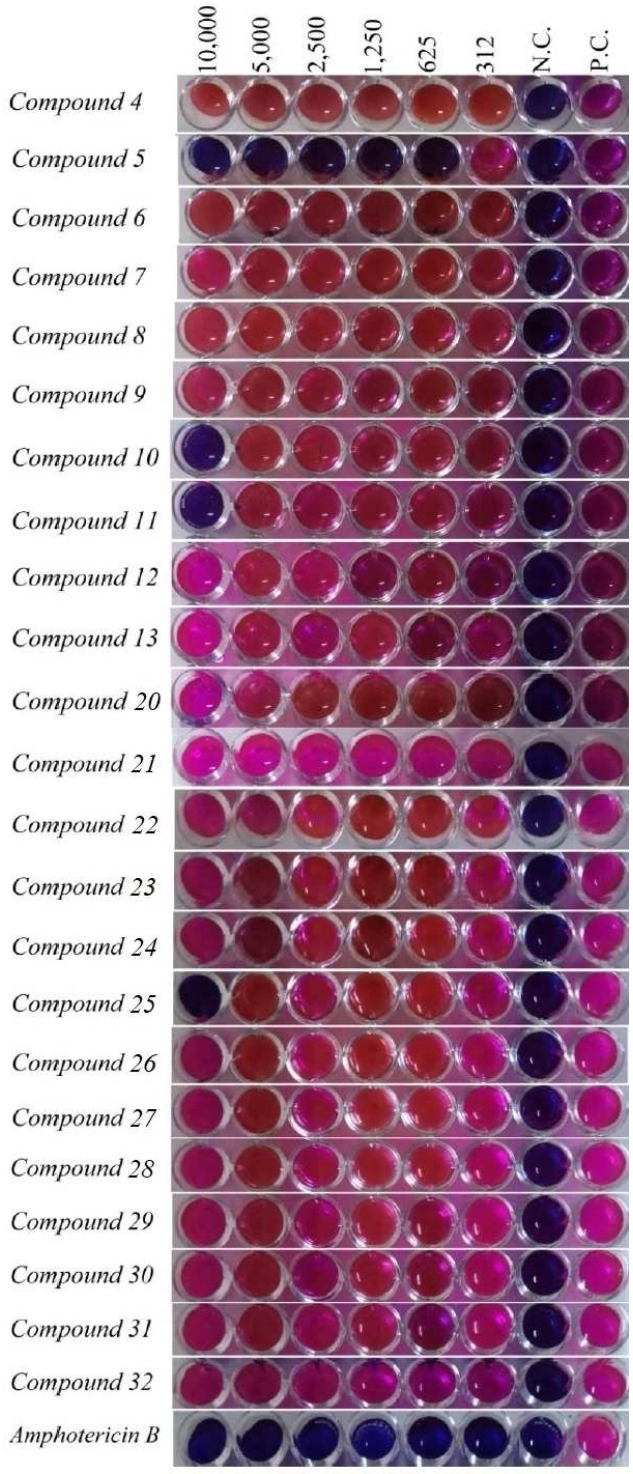

Figure 1. The antileishmanial activity results against axenic standard *Leishmania infantum* promastigotes; Control drug: Amphotericin B. Dilution concentrations: 10,000-312 μg/mL. N.C.: Negative Control; P.C.: Positive Control.

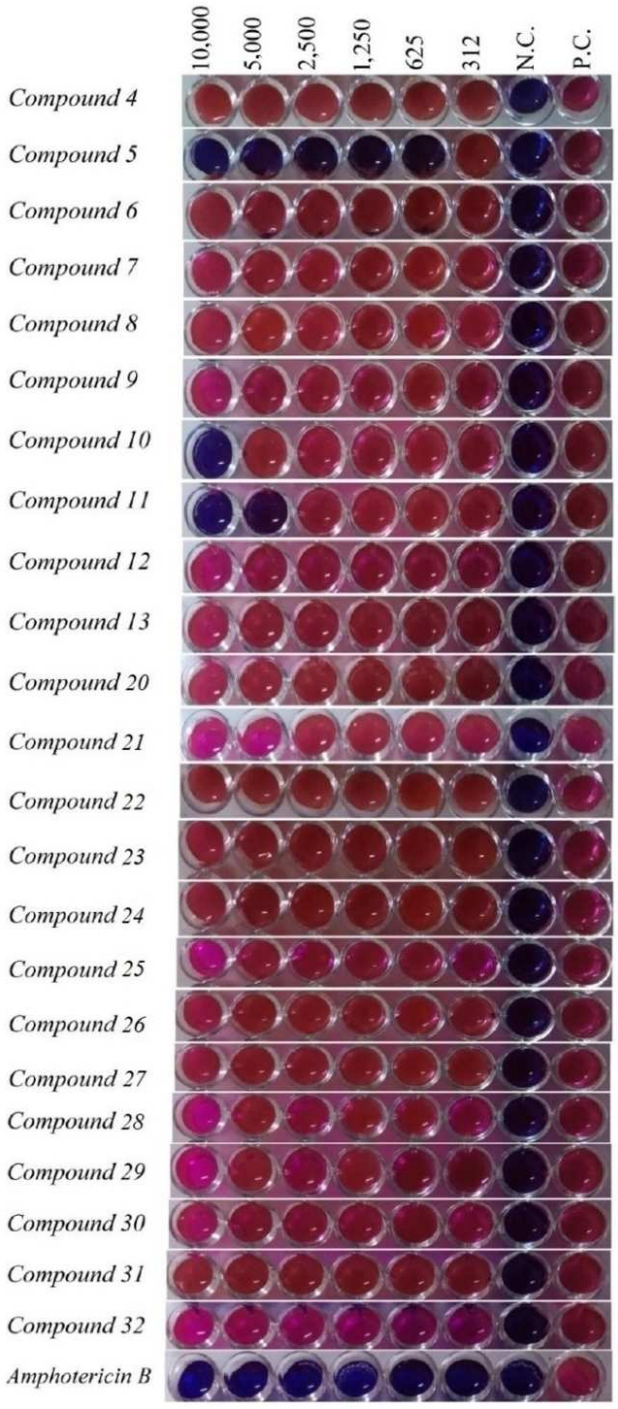

Figure 2. The antileishmanial activity results against axenic standard *Leishmania tropica* promastigotes; Control drug: Amphotericin B. Dilution concentrations: 10,000-312 μg/mL. N.C.: Negative Control; P.C.: Positive Control.

pharmacokinetics and toxicity analyses with Lipinski and FAF-Drugs standards. In addition, it is aimed to investigate the inhibiting effect of all compounds on the 3JUS *Escherichia coli* receptor using molecular docking simulation.

Scheme 1 shows the synthetic route used to synthesize the imidazo[2,1-*b*][1,3,4]thiadiazole derivatives (**4-13** and **20–32**).

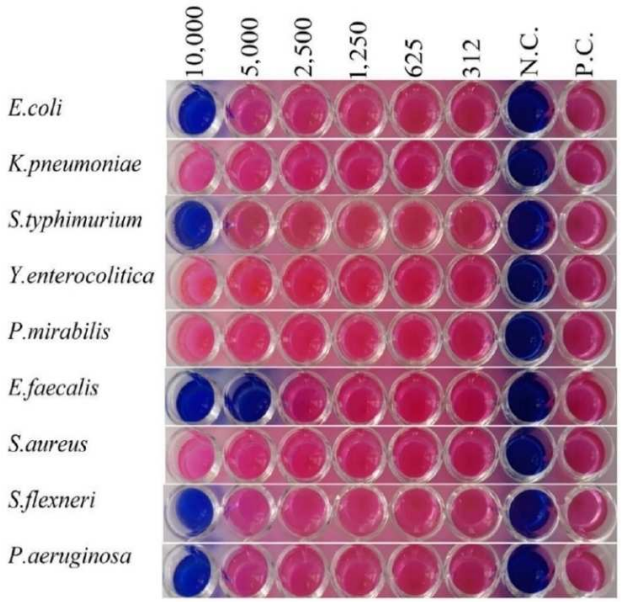

Figure 3. The antibacterial activity results of compound **25**; dilution concentrations 10,000-312 µg/mL. N.C.: Negative Control; P.C.: Positive Control.

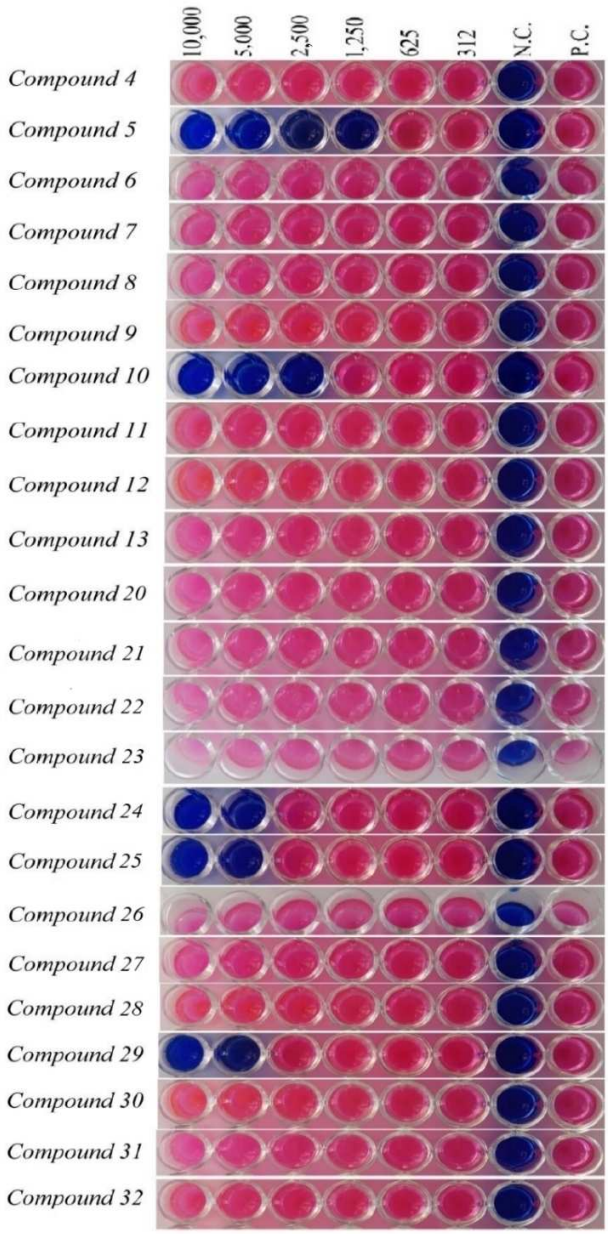

Figure 4. The antibacterial activity results of the compounds against *Enterococcus faecalis*; dilution concentrations 10,000-312 µg/mL. N.C.: Negative Control; P.C.: Positive Control.

Results and Discussion

Chemistry

In this study, the substituted imidazo[2,1-*b*][1,3,4]thiadiazole derivatives (**4-13** and **20–32**), the target compounds, were obtained using the synthetic pathway shown in Scheme 1.

In the first part of the study, 5-(4-fluorobenzylthio)-1,3,4-thiadiazole-2-amine (**3**), the initial compound, was synthesized from the reaction of 4-fluorobenzylchloride (**1**) with 2-amino-5-mercapto-1,3,4-thiadiazole (**2**) in the presence of KOH. Compounds **1** and **2**, which were used as initial compounds, were obtained commercially, while compound **3** was obtained as specified in the literature.[1,16,17]

In the second part of the study, the other 2-amino-1,3,4-thiadiazole derivatives (**17-19**) were synthesized from the reaction of 4-substituted phenylacetonitrile derivatives (**14-16**) with thiosemicarbazide in trifluoroacetic acid (TFA) in high yields. 4-Substituted phenylacetonitrile derivatives used as initial compounds (**14-16**) were obtained commercially, while 2-amino-1,3,4-thiadiazole derivatives were obtained as specified in the literature.[21]

In this reaction, the nucleophilic attack of thiosemicarbazide to the imine carbon occurs first under the catalytic effect of TFA. It is believed that the elimination of the ammonia ion and the sulfur's nucleophilic attack on the carbon atom result in a heterocyclization, which leads to the formation of 2-amino-1,3,4-thiadiazole derivatives.[21] Scheme 2 shows the reaction mechanism.

In this study, we synthesized the imidazo[2,1-*b*][1,3,4] thiadiazole derivatives (**4-13** and **20–32**), the target compounds, from the reactions of 2-amino-1,3,4-thiadiazole derivatives with various phenacyl bromide derivatives in moderate-good yields ranging from 59% to 77%. The mechanism proposed for the formation of these compounds can be seen in Scheme 3 and Scheme 4.

The most significant evidence for the formation of the imidazo[2,1-*b*][1,3,4]thiadiazole derivatives (**4-13** and **20–32**) is the disappearance of the -NH_2 group's symmetric and asymmetric absorption bands found in the initial compounds (**3**, **17–19**) and observed in the 3265–3070 cm^{-1} range in the IR spectra.

Additionally, there are two significant pieces of evidence for the formation of these compounds in the ^{1}H NMR spectra. The first is the disappearance of the -NH_2 group proton signals

Table 2. Minimum inhibitory concentration (MIC) values of all compounds against bacteria.

Compounds	*Escherichia coli*	*Klebsiella pneumoniae*	*Salmonella typhimurium*	*Yersinia enterocolitica*	*Proteus mirabilis*	*Enterococcus faecalis*	*Staphylococcus aureus (MRSA)*	*Shigella flexneri*	*Pseudomonas aeruginosa*
4	>10,000	>10,000	>10,000	>10,000	>10,000	>10,000	>10,000	>10,000	>10,000
5	10,000	>10,000	10,000	>10,000	>10,000	1,250	>10,000	>10,000	>10,000
6	>10,000	>10,000	>10,000	>10,000	>10,000	>10,000	>10,000	>10,000	>10,000
7	>10,000	>10,000	>10,000	>10,000	>10,000	>10,000	>10,000	>10,000	>10,000
8	>10,000	>10,000	>10,000	>10,000	>10,000	>10,000	>10,000	>10,000	>10,000
9	>10,000	>10,000	>10,000	>10,000	>10,000	>10,000	>10,000	>10,000	>10,000
10	5,000	>10,000	>10,000	>10,000	>10,000	2,500	>10,000	5,000	>10,000
11	>10,000	>10,000	>10,000	>10,000	>10,000	>10,000	>10,000	>10,000	>10,000
12	>10,000	>10,000	>10,000	>10,000	>10,000	>10,000	>10,000	>10,000	>10,000
13	>10,000	>10,000	>10,000	>10,000	>10,000	>10,000	>10,000	>10,000	>10,000
20	>10,000	>10,000	>10,000	>10,000	>10,000	>10,000	>10,000	>10,000	>10,000
21	>10,000	>10,000	>10,000	>10,000	>10,000	>10,000	>10,000	>10,000	>10,000
22	>10,000	>10,000	>10,000	>10,000	>10,000	>10,000	>10,000	>10,000	>10,000
23	>10,000	>10,000	>10,000	>10,000	>10,000	>10,000	>10,000	>10,000	>10,000
24	10,000	>10,000	10,000	>10,000	>10,000	5,000	>10,000	>10,000	10,000
25	10,000	>10,000	10,000	>10,000	>10,000	5,000	>10,000	10,000	10,000
26	>10,000	>10,000	>10,000	>10,000	>10,000	>10,000	>10,000	>10,000	>10,000
27	>10,000	>10,000	>10,000	>10,000	>10,000	>10,000	>10,000	>10,000	>10,000
28	>10,000	>10,000	>10,000	>10,000	>10,000	>10,000	>10,000	>10,000	>10,000
29	>10,000	>10,000	>10,000	10,000	>10,000	5,000	>10,000	2,500	10,000
30	>10,000	>10,000	>10,000	>10,000	>10,000	>10,000	>10,000	>10,000	>10,000
31	>10,000	>10,000	>10,000	>10,000	>10,000	>10,000	>10,000	>10,000	>10,000
32	>10,000	>10,000	>10,000	>10,000	>10,000	>10,000	>10,000	>10,000	>10,000

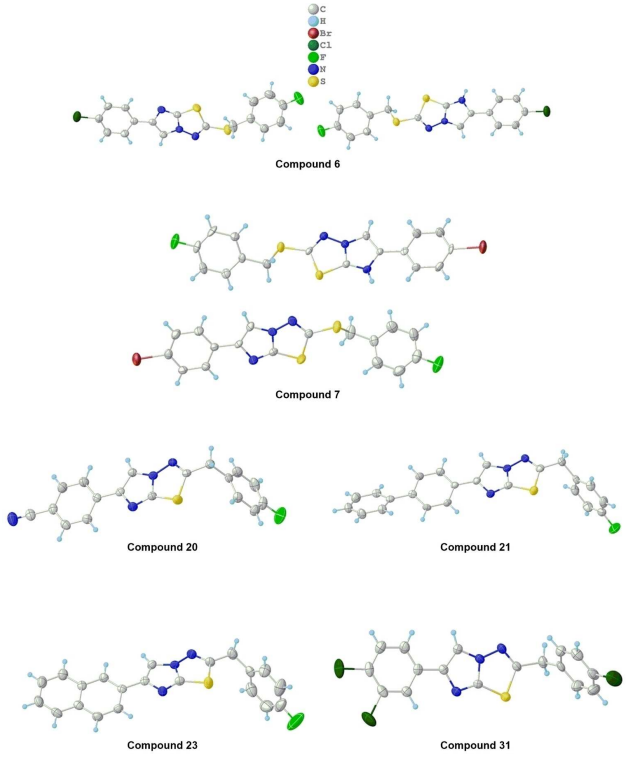

Figure 5. The crystal structures of compounds **6**, **7**, **20**, **21**, **23**, and **31**.

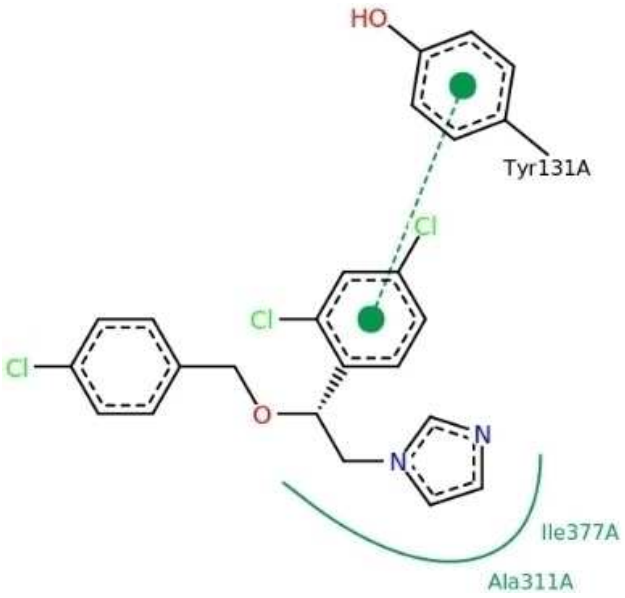

Figure 6. The interactions between the 3JUS receptor and econazole.

corresponding to 2 protons and observed at 7.28-7.04 ppm for the 2-amino-1,3,4-thiadiazole derivatives, the initial compounds. The second is the observation of a singlet corresponding to 1 proton in the 8.94-8.48 ppm range, representing C_5-H signals in the imidazo[2,1-*b*][1,3,4]thiadiazole derivatives. This is consistent with studies in the literature.[1,17, 21] Other ^{1}H NMR data of these compounds are given in the experimental part of this study in detail (supporting information section).

The carbon signals that appeared in the 113.70-109.94 ppm range and the 146.54-145.07 ppm range in the ^{13}C NMR spectra of the imidazo[2,1-*b*][1,3,4]thiadiazole derivatives are important evidence of ring cyclization. These signals correspond to the C_5 and C_6 carbons of imidazo[2,1-*b*][1,3,4]thiadiazole derivatives, the target compounds. Other ^{13}C NMR spectral data of these

Table 3. Crystallographic data for compounds **6**, **7**, **20**, **21**, **23**, and **31**.

Compounds	6	7	20	21	23	31
Molecular formula	$C_{17}H_{11}ClFN_3S_2$	$C_{17}H_{11}BrFN_3S_2$	$C_{18}H_{11}FN_4S$	$C_{23}H_{16}FN_3S$	$C_{21}H_{14}FN_3S$	$C_{17}H_{10}Cl_3N_3S$
Molecular weight	376.87	420.82	334.43	385.45	359.41	394.71
Temperature/K	293(2)	293(2)	293	293(2)	293(2)	293
Crystal system	triclinic	triclinic	monoclinic	monoclinic	monoclinic	triclinic
Space group	P-1	P-1	$P2_1/n$	$P2_1/n$	$P2_1/n$	P-1
a/Å	8.3803(6)	8.3060(8)	7.1646(6)	11.3199(12)	5.6071(6)	7.2220(8)
b/Å	12.6511(8)	12.9165(14)	16.2179(16)	6.2033(7)	17.0197(19)	7.4430(8)
c/Å	16.0206(11)	16.0826(17)	13.1568(13)	26.201(3)	17.820(2)	16.0726(18)
α/°	99.035(2)	100.219(5)	90	90	90	81.416(5)
β/°	92.053(3)	92.548(5)	94.259(3)	92.180(4)	93.959(5)	84.683(5)
γ/°	106.185(2)	106.566(5)	90	90	90	79.937(5)
Volume/$Å^3$	1605.26(19)	1619.3(3)	1524.5(3)	1838.5(3)	1696.5(3)	839.17(16)
Z	4	4	4	4	4	2
ρcalcg/cm^3	1.559	1.726	1.4570	1.393	1.407	1.5620
μ/mm^{-1}	0.512	2.810	0.230	0.199	0.210	0.674
F(000)	772.0	842.0	688.9	800.0	744.0	401.2
Crystal size/mm^3	0.21 × 0.17 × 0.16	0.16 × 0.15 × 0.12	0.23 × 0.19 × 0.18	0.15 × 0.1 × 0.09	0.22 × 0.18 × 0.15	0.23 × 0.18 × 0.15
Radiation	MoKα (λ = 0.71073)	MoKα (λ = 0.71073)	Mo Kα (λ = 0.71073)	MoKα (λ = 0.71073)	MoKα (λ = 0.71073)	Mo Kα (λ = 0.71073)
2Θ range for compound data collection/°	5.89 to 56.766	5.776 to 52	5.9 to 52	5.786 to 49.992	6.628 to 49.998	5.74 to 51.98
Index ranges	-11 ≤ h ≤ 11, −16 ≤ k ≤ 16, −21 ≤ l ≤ 21	-10 ≤ h ≤ 10, −15 ≤ k ≤ 15, −19 ≤ l ≤ 19	-9 ≤ h ≤ 8, −21 ≤ k ≤ 21, −17 ≤ l ≤ 17	-13 ≤ h ≤ 13, −7 ≤ k ≤ 7, −31 ≤ l ≤ 31	-6 ≤ h ≤ 6, −20 ≤ k ≤ 20, −21 ≤ l ≤ 21	-9 ≤ h ≤ 10, −10 ≤ k ≤ 10, −22 ≤ l ≤ 22
Reflections collected	74129	40804	31810	34994	56326	36628
Independent reflections	8010 [R_{int} = 0.0315, R_{sigma} = 0.0172]	6272 [R_{int} = 0.0855, R_{sigma} = 0.0581]	2956 [R_{int} = 0.0434, R_{sigma} = 0.0292]	3199 [R_{int} = 0.0607, R_{sigma} = 0.0361]	2984 [R_{int} = 0.0513, R_{sigma} = 0.0218]	3248 [R_{int} = 0.0566, R_{sigma} = 0.0572]
Data/restraints/parameters	8010/0/434	6272/0/434	2956/6/237	3199/0/253	2984/0/236	3248/0/217
Goodness-of-fit on F^2	1.088	1.319	1.065	1.025	1.199	1.066
Final R indexes [I > = 2σ (I)]	R_1 = 0.0508, wR_2 = 0.0930	R_1 = 0.1002, wR_2 = 0.1692	R_1 = 0.0660, wR_2 = 0.1721	R_1 = 0.0986, wR_2 = 0.2113	R_1 = 0.0991, wR_2 = 0.2014	R_1 = 0.0858, wR_2 = 0.1821
Final R indexes [all data]	R_1 = 0.0694, wR_2 = 0.1059	R_1 = 0.1238, wR_2 = 0.1775	R_1 = 0.0740, wR_2 = 0.1799	R_1 = 0.1100, wR_2 = 0.2167	R_1 = 0.1035, wR_2 = 0.2029	R_1 = 0.0984, wR_2 = 0.1884
Largest diff. peak/hole / e $Å^{-3}$	0.31/-0.74	0.66/-0.66	0.46/-0.53	0.27/-0.35	0.32/-0.27	0.81/-0.64
CCDC	1538525	1538527	1538532	1538529	1538524	1538530

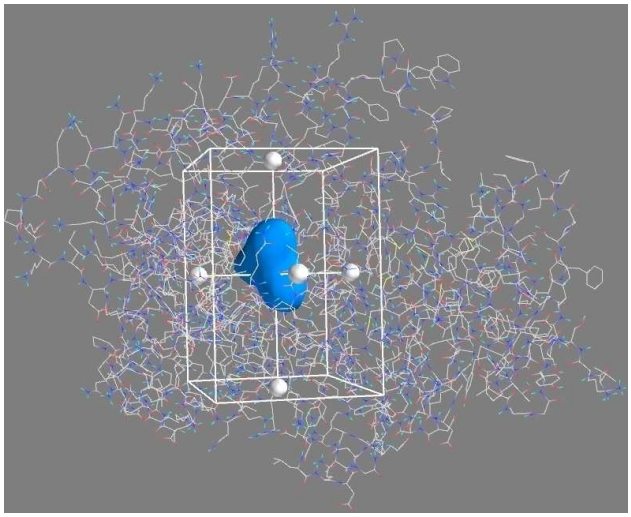

Figure 7. The position of the co-ligand in the active site of the 3JUS receptor.

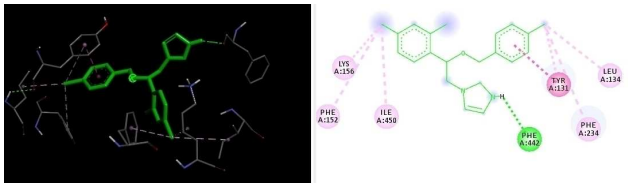

Figure 8. The 3D and 2D presentation of docking results of the co-ligand in the active region of the 3JUS receptor.

Figure 9. The 3D and 2D presentation of docking results of ligand **10** in the active region of the 3JUS receptor.

Table 4. The pharmacological properties of virtual screening and rationally designed ligands.

Comp.	Binding affinity	MW	logP	TPSA	Rotatable Bonds	Flexibility	HBD	HBA	Lipinski Violation	Solubility (mg/l)	Predicted LD50 mg/kg	Predicted Toxicity Class
4	-8.9	341.43	4.95	83.73	4	0.16	0	3	0	1859.07	300	3
5	-9.0	361.43	5.39	78.23	4	0.16	1	3	1	1548.82	300	3
6	-10.4	375.87	5.58	83.73	4	0.16	0	3	1	1111.52	300	3
7	-8.7	420.32	5.64	83.73	4	0.16	0	3	1	908.57	300	3
8	-10.1	371.45	4.92	92.96	5	0.19	0	4	0	1904.66	300	3
9	-9.1	386.42	4.78	129.55	5	0.18	0	6	0	1934.23	1000	4
10	-9.0	366.44	4.67	107.52	4	0.15	0	4	0	2061.16	300	3
11	-10.1	417.52	6.57	83.73	5	0.16	0	3	1	540.91	300	3
12	-9.0	410.32	6.2	83.73	4	0.16	0	3	1	663.16	300	3
13	-10.1	391.48	6.2	83.73	4	0.13	0	3	1	701.61	300	3
20	-9.0	334.37	4.29	82.22	3	0.12	0	4	0	2698.62	300	3
21	-10.1	385.46	6.19	58.43	4	0.13	0	3	1	717.81	300	3
22	-9.0	378.25	5.82	58.43	3	0.13	0	3	1	876.58	300	3
23	-10.0	359.42	5.82	58.43	3	0.1	0	3	1	924.95	300	3
24	-8.9	339.39	4.54	67.66	4	0.16	0	4	0	2501.13	300	3
25	-8.9	346.41	4.16	91.45	4	0.15	0	5	0	3134.85	300	3
26	-9.5	397.49	6.06	67.66	5	0.16	0	4	1	824.9	300	3
27	-8.9	390.29	5.69	67.66	4	0.16	0	4	1	1016.54	300	3
28	-8.9	371.45	5.69	67.66	4	0.13	0	4	1	1069.18	300	3
29	-9.5	350.82	4.81	82.22	3	0.12	0	4	0	1842.57	300	3
30	-10.1	401.91	6.72	58.43	4	0.13	0	3	1	484	300	3
31	-8.9	394.71	6.35	58.43	3	0.13	0	3	1	591.52	300	3
32	-8.8	375.87	6.34	58.43	3	0.1	0	3	1	629.48	300	3
Co-ligand	-7.9	381.68	5.3	27.05	6	0.26	0	3	1	1604.14	463	4

The properties are PhysChem and FAFDrugs filters. HBD: hydrogen bonds donor; HBA: hydrogen bond acceptor; TPSA: topological polar surface area; LogP: indicator of hydrophobicity.

Table 5. The interactions between the co-ligand and the 3JUS receptor.

Name	Distance Donor…Acceptor (Å)	Interaction Category	Interaction Types	Donor group	Donor group Types	Acceptor group	Acceptor group Types
N:UNK1:HN - A:PHE442:O	2.152	Hydrogen Bond	Conventional Hydrogen Bond	N:UNK1:HN	H-Donor	A:PHE442:O	H-Acceptor
A:TYR131 - N:UNK1	3.685	Hydrophobic	Pi–Pi Stacked	A:TYR131	Pi-Orbitals	N:UNK1	Pi-Orbitals
N:UNK1:Cl - A:LEU134	4.040	Hydrophobic	Alkyl	N:UNK1:Cl	Alkyl	A:LEU134	Alkyl
N:UNK1:Cl - A:LYS156	4.082	Hydrophobic	Alkyl	N:UNK1:Cl	Alkyl	A:LYS156	Alkyl
N:UNK1:Cl - A:ILE450	4.664	Hydrophobic	Alkyl	N:UNK1:Cl	Alkyl	A:ILE450	Alkyl
A:TYR131 - N:UNK1:Cl	4.884	Hydrophobic	Pi-Alkyl	A:TYR131	Pi-Orbitals	N:UNK1:Cl	Alkyl
A:PHE152 - N:UNK1:Cl	4.786	Hydrophobic	Pi-Alkyl	A:PHE152	Pi-Orbitals	N:UNK1:Cl	Alkyl
A:PHE234 - N:UNK1:Cl	5.059	Hydrophobic	Pi-Alkyl	A:PHE234	Pi-Orbitals	N:UNK1:Cl	Alkyl

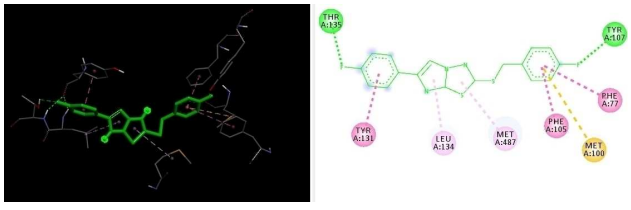

Figure 10. The 3D and 2D presentation of docking results of ligand **5** in the active region of the 3JUS receptor.

compounds are given in the experimental part of this study in detail (supporting information section).

The FT-IR, ^{1}H NMR, ^{13}C NMR, elemental, and mass spectroscopy analyses of all the compounds synthesized in this study can be found in the experimental section and all the spectra are given in the supporting information section in detail.

In vitro Antileishmanial Activity Studies

We determined the *in vitro* antileishmanial activities of the compounds against *Leishmania infantum* and *Leishmania*

Table 6. The interactions between ligand **10** and the 3JUS receptor.

Name	Distance Donor… Acceptor (Å)	Interaction Category	Interaction Types	Donor group	Donor group Types	Acceptor group	Acceptor group Types
A:MET100:SD - N:UNK1	5.300	Other	Pi-Sulfur	A:MET100:SD	Sulfur	N:UNK1	Pi-Orbitals
A:PHE77 - N:UNK1	5.227	Hydrophobic	Pi–Pi Stacked	A:PHE77	Pi-Orbitals	N:UNK1	Pi-Orbitals
A:PHE105 - N:UNK1	4.142	Hydrophobic	Pi–Pi Stacked	A:PHE105	Pi-Orbitals	N:UNK1	Pi-Orbitals
A:TYR131 - N:UNK1	3.821	Hydrophobic	Pi–Pi Stacked	A:TYR131	Pi-Orbitals	N:UNK1	Pi-Orbitals
N:UNK1 - A:MET487	5.301	Hydrophobic	Pi-Alkyl	N:UNK1	Pi-Orbitals	A:MET487	Alkyl

Table 7. The interactions between ligand **5** and the 3JUS receptor.

Name	Distance Donor… Acceptor (Å)	Interaction Category	Interaction Types	Donor group	Donor group Types	Acceptor group	Acceptor group Types
A:TYR107:HH - N:UNK1:F	2.128	Hydrogen Bond; Halogen	Conventional Hydrogen Bond; Halogen (Fluorine)	A:TYR107:HH	H-Donor; Halogen Acceptor	N:UNK1:F	H-Acceptor; Halogen
A:THR135:HG1 -N:UNK1:F	2.839	Hydrogen Bond; Halogen	Conventional Hydrogen Bond; Halogen (Fluorine)	A:THR135:HG1	H-Donor; Halogen Acceptor	N:UNK1:F	H-Acceptor; Halogen
A:MET100:SD - N:UNK1	5.264	Other	Pi-Sulfur	A:MET100:SD	Sulfur	N:UNK1	Pi-Orbitals
A:PHE77 - N:UNK1	5.226	Hydrophobic	Pi–Pi Stacked	A:PHE77	Pi-Orbitals	N:UNK1	Pi-Orbitals
A:PHE105 - N:UNK1	4.202	Hydrophobic	Pi–Pi Stacked	A:PHE105	Pi-Orbitals	N:UNK1	Pi-Orbitals
A:TYR131 - N:UNK1	3.923	Hydrophobic	Pi–Pi Stacked	A:TYR131	Pi-Orbitals	N:UNK1	Pi-Orbitals
N:UNK1 - A:MET487	5.235	Hydrophobic	Pi-Alkyl	N:UNK1	Pi-Orbitals	A:MET487	Alkyl
N:UNK1 - A:LEU134	5.059	Hydrophobic	Pi-Alkyl	N:UNK1	Pi-Orbitals	A:LEU134	Alkyl

tropica promastigotes using the microdilution Alamar blue assay method. Figure 1 and Figure 2 show the antileishmanial activity test results of the synthesized compounds and Table 1 shows the minimum inhibitory concentration (MICs) values. The negative and positive control wells were detected to work properly.

The antileishmanial activity tests showed that the most effective compound against the *Leishmania infantum* promastigotes was compound **5** (MIC: 625 μg/mL). Compounds **10**, **11**, and **25** were also found to be effective at the highest concentration studied (MIC: 10,000 μg/mL). Other compounds had no antileishmanial activity against *Leishmania infantum* promastigotes at the studied concentrations.

The most effective compound against the *Leishmania tropica* promastigotes was compound **5** as well (MIC: 625 μg/mL). Compound **10** was found to be effective at the highest concentration studied (MIC: 10,000 μg/mL), while compound **11** was found to be effective at a lower concentration (MIC: 5,000 μg/mL). Other compounds had no antileishmanial activity against *Leishmania tropica* promastigotes at the studied concentrations. Amphotericin B, the standard drug, was found to be effective at a concentration of <312 μg/mL.

In vitro Antibacterial Activity Studies

In vitro antibacterial activity of bacteria was performed by microdilution broth method against nine different bacteria isolates (7 Gram-negative, 2 Gram-positive).

Some of the synthesized compounds were found to have different concentrations of antibacterial activity against standard bacterial isolates, while some compounds were found to be ineffective at the studied concentrations. Antibacterial activity images of some compounds are shown in Figure 3 and Figure 4. The MIC values of the compounds were presented in Table 2.

The antibacterial activity studies showed that the synthesized compounds were effective against six out of nine standard bacterial isolates at varying concentrations. The compounds were most effective against *E. faecalis* at different concentrations (MIC: 1,250-5,000 μg/mL). Compound **25** was found to be effective against the highest number of bacterial species (five species) (Figure 3). Compounds **5**, **10**, **24**, **25**, and **29** were found to have antibacterial activity. The compounds had no antibacterial activity against three of the bacterial species at any concentration studied, namely *S. aureus* (MRSA), *K. pneumoniae*, and *P. mirabilis*. Compounds **5**, **10**, and **25** were found to have both antibacterial and antileishmanial activity.

The structure-activity relationship (SAR) was also investigated. Electron withdrawing and electron donating groups such as 4-fluorophenyl, 4-chlorophenyl, 4-methoxyphenyl were chosen as the R′ groups in the SAR study. Then, electron donating groups such as methoxy, phenyl, and naphthyl and electron withdrawing groups such as nitro, cyano, fluoro, chloro, and bromo groups were chosen as substituents and as the R groups to confer the effect of different electronic environments on the activities.

It was observed that the R′ groups (4-fluorophenyl, 4-chlorophenyl and 4-methoxyphenyl) had no significant effect on activity in general. However, significant increases in activity were observed in the presence of electron withdrawing and less bulky groups such as cyano and fluoro used as R groups (Tables 1 and 2). On the other hand, the presence of electron donating and bulky groups such as phenyl and naphthyl was observed to significantly decrease the activity. These results are also consistent with the literature.[1,21]

Crystallographic Analysis Studies

Single crystals of compounds **6**, **7**, **20**, **21**, **23**, and **31** were obtained and their structures were confirmed by X-ray analysis. Not all crystals had classical hydrogen bonds and the packaging of the crystals occurred with weak van der Waals and π-π interactions. Crystals **6** and **7** were formed by two molecules in the asymmetrical unit. Table 3 and Figure 5 show the crystallographic data and the crystal structures of the compounds (**6**, **7**, **20**, **21**, **23**, and **31**), respectively. Bond lengths, bond angles, and packing structures of compounds **6**, **7**, **20**, **21**, **23**, and **31** are given in the supporting information section.

Pharmacological Properties and Molecular Docking Studies

The molecular weight (MW), the percentage of human oral absorption, the indicator of hydrophobicity (logP), the topological polar surface area (TPSA), and the violation of the Lipinski rule[22] were calculated for all compounds, which can be seen in Table 4. The results showed that most of the active compounds, especially the ligands with experimental activity (**10**, **24**, **25**, and **29**), did not violate the Lipinski rule. This indicates a molecule's drug similarity. The TPSA values (recommended value: $\leq$140 Å^2)[23] were within the recommended range. As a result of the analysis, ligand **9** was classified as class 4 (LD50 of 1000 mg/kg) and the other ligands were classified as class 3 in terms of oral toxicity level (1: the most toxic; 6: the safest).[24] This indicates that ligand **9**, which has a low toxicity value, may be considered as a candidate drug for *in vitro* studies. Table 4 shows the pharmacological properties of the ligands as well as their binding affinity. Ligands **5**, **10**, **24**, and **25**, which were effective in *in vitro* studies, were observed to have high binding affinity.

The protein structure of the lanosterol 14α-demethylase (CYP51) enzyme (PDB ID: 3JUS), which plays a significant role in sterol biosynthesis in fungi and is a vital antimicrobial drug target,[25] was used in molecular docking studies. Econazole, an antifungal drug that inhibits this enzyme, was used as the co-ligand. Figure 6 shows the interactions between the 3JUS receptor and econazole, which were illuminated by X-ray diffraction.[26]

The 3JUS receptor and all ligand compounds were prepared for docking using protein and ligand preparation wizards in the PyRx package.[22] In this step, the position of the co-ligand in the 3JUS protein was identified with a white grid box (center_x = 42.175, center_y = 5.48080384326, center_z = 47.4573031795, size_x = 16.2300265022, size_y = 18.0459550143, size_z = 23.966) in 3D view as shown below (Figure 7). This grid box allows for selection of the search site for all ligands in the protein.

Molecular docking studies were performed to see possible binding modes of all synthesized compounds and co-ligand. Docking scores of all compounds and co-ligand molecule can be seen in Table 4. Figures 8 to 10 show the 3D representation of the co-ligand, ligand **5**, and ligand **10** located in the active binding sites of the target protein and Tables 5 to 7 show the interactions between the ligands and the receptor. These three ligands were observed to interact with the TYR131 residue in the active binding site of the receptor and the interaction distance of the co-ligand was 4.884 Å, while the interaction distance for ligands 5 and 10, which had shorter interaction distances, was 3.923 and 3.821 Å, respectively. As can be seen in Table 4, the interaction distance of these three ligands with the TYR131 residue was directly proportional to their docking scores. The ligands were also observed to bond with alkyl and hydrophobic interactions.

Conclusions

In this study, imidazo[2,1-*b*][1,3,4]thiadiazole derivatives, the target compounds of this study containing both imidazole and 1,3,4-thiadiazole rings, were synthesized using simple reaction methods and under mild reaction conditions. The structures of the synthesized compounds were illuminated using a variety of analysis techniques such as FT-IR, ^{1}H NMR, ^{13}C NMR, mass spectroscopy, X-ray diffraction, and elemental analyses.

All compounds were tested for *in vitro* antileishmanial and antibacterial activity. According to the results of the biological activity tests, some compounds had moderate-high levels of biological activity.

The molecular docking studies showed that all ligands had higher docking scores compared to the 3JUS receptor and econazole, the inhibitor of this receptor, and had interactions similar to those of econazole. The docking scores of compounds **5**, **10**, **24**, **25**, and **29**, which showed moderate to good antibacterial activity, were found to be −9.0, −9.0, −8.9, −8.9, and −9.5, respectively. Compounds **10**, **24**, **25**, and **29** were compliant with the Lipinski rules and pharmacological filters such as FAF-Drugs.

Supporting Information Summary

The supporting information contains details of the experimental procedures (synthetic, biological and theoretical), spectral

characterization data for all compounds and X-Ray data for compounds **6**, **7**, **20**, **21**, **23** and **31**.

We would like to thank Karabuk University Scientific Research Fund (Project ID Number: KBUBAP-18-YL-012) for funding this project.

Keywords: Ab initio calculations · ADME · Biological activity · Imidazo[2,1-*b*][1,3,4]thiadiazole · Molecular docking.

[1] H. Tahtaci, H. Karacık, A. Ece, M. Er, M. G. Şeker, *Mol. Inf.* **2018**, *37*, 1700083.
[2] S. G. Alegaon, K. R. Alagawadi, *Eur. J. Chem.* **2011**, *2*, 94–99.
[3] Lata, K. Kushwaha, A. Gupta, D. Meeana, A. Verma, *Heterocycl. Lett.* **2015**, *5*, 489–509.
[4] Y. Luo, S. Zhang, Z. J. Liu, W. Chen, J. Fu, Q. F. Zeng, H. L. Zhu, *Eur. J. Med. Chem.* **2013**, *64*, 54–61.
[5] B. Chandrakantha, A. M. Isloor, P. Shetty, H. K. Fun, G. Hedge, *Eur. J. Med. Chem.* **2014**, *71*, 316–323.
[6] K. F. M. Atta, O. O. M. Farahat, A. Z. A. Ahmed, M. G. Marei, *Molecules* **2011**, *16*, 5496–5506.
[7] A. A. Kadi, N. R. El-Brollosy, O. A. Al-Deeb, E. E. Habib, T. M. Ibrahim, A. A. El-Emam, *Eur. J. Med. Chem.* **2007**, *42*, 235–242.
[8] A. K. Gadad, M. B. Palkar, K. Anand, M. N. Noolvi, T. S. Boreddy, J. Wagwade, *Bioorg. Med. Chem.* **2008**, *16*, 276–283.
[9] V. B. Jadhav, M. V. Kulkarni, V. P. Rasal, S. S. Biradar, M. D. Vinay, *Eur. J. Med. Chem.* **2008**, *43*, 1721–1729.
[10] J. Ramprasad, N. Nayak, U. Dalimba, P. Yogeeswari, D. Sriram, *Bioorg. Med. Chem. Lett.* **2015**, *25*, 4169–4173.
[11] J. Ramprasad, N. Nayak, U. Dalimba, P. Yogeeswari, D. Sriram, S. K. Peethambar, R. Achur, H. S. Kumar, *Eur. J. Med. Chem.* **2015**, *95*, 49–63.
[12] S. G. Alegaon, K. R. Alagawadi, P. V. Sonkusare, S. M. Chaudhary, D. H. Dadwe, A. S. Shah, *Bioorg. Med. Chem. Lett.* **2012**, *22*, 1917–1921.
[13] A. K. Gadad, M. N. Noolvi, R. V. Karpoormath, *Bioorg. Med. Chem.* **2004**, *12*, 5651–5659.
[14] A. I. Khazi, C. S. Mahajanshetti, A. K. Gadad, A. D. Tarnalli, C. M. Sultanpur, *Arzneim.-Forsch.* **1996**, *46*, 949–952.
[15] A. Andreani, M. Rambaldi, G. Mascellani, P. Rugarli, *Eur. J. Med. Chem.* **1987**, *22*, 19–22.
[16] M. Er, H. Tahtaci, T. Karakurt, A. Onaran, *J. Heterocycl. Chem.* **2019**, *56*, 2555–2570.
[17] M. Er, A. Özer, Ş. Direkel, T. Karakurt, H. Tahtaci, *J. Mol. Struct.* **2019**, *1194*, 284–296.
[18] Q. Jiang, J. Chen, C. Yang, Y. Yin, K. Yao, *BioMed Res. Int.* **2019**, *2019*, 2015978. doi: 10.1155/2019/2015978.
[19] P. S. Yadav, Devprakash, G. P. Senthilkumar, *Int. J. Pharm. Sci. Drug Res.* **2011**, *3*, 1–7.
[20] World Health Organization (WHO) "Leishmaniasis" to be found under https://www.who.int/news-room/fact-sheets/detail/leishmaniasis, **2019**.
[21] M. Er, B. Ergüven, H. Tahtaci, A. Onaran, T. Karakurt, A. Ece, *Med. Chem. Res.* **2017**, *26*, 615–630.
[22] C. A. Lipinski, F. Lombardo, B. W. Dominy, P. J. Feeney, *Adv. Drug Delivery Rev.* **1997**, *23*, 3–25.
[23] D. F. Veber, S. R. Johnson, H.-Y. Cheng, *J. Med. Chem.* **2002**, *45*, 2615–2623.
[24] B. Rashidieh, Z. Madani, M. K. Azam, S. K. Maklavani, N. R. Akbari, S. Tavakoli, G. Rigi, *Bioinformation*, **2015**, *11*, 501–505.
[25] F. Chioma, A. C. Ekennia, C. U. Ibeji, S. N. Okafor, D. C. Onwudiwe, A. A. Osowole, O. T. Ujam, *J. Mol. Struct.* **2018**, *1163*, 455–464.
[26] N. Strushkevich, S. A. Usanov, H. W. Park, *J. Mol. Biol.* **2010**, *397*, 1067–1078.

Submitted: October 15, 2019
Accepted: December 9, 2019